Available online at www.sciencedirect.com

SciVerse ScienceDirect

Journal of the European Ceramic Society 32 (2012) 2859–2866

www.elsevier.com/locate/jeurceramsoc

Wetting and corrosion of yttria stabilized zirconia by molten slags

Yannick Hemberger*, Christoph Berthold, Klaus G. Nickel

University of Tübingen, Faculty of Science, Department of Geosciences, Applied Mineralogy, Wilhelmstraße 56, D-72074 Tübingen, Germany

Available online 2 January 2012

Abstract

We present first results of a study dealing with the corrosion of yttria stabilized zirconia ceramics by molten slags. Good wetting of a typical metallurgical slag as a pre-requisite for an effective chemical interaction of melt and zirconia was found. Both the dissolution of Zirconia and the leaching of the stabilizing agent into the molten slag are observed corrosion mechanisms. The latter induces a phase transformation from tetragonal or cubic zirconia into the monoclinic modification. The transformation with its increase in volume by app. 5% induces cracks. Those act to give new pathways for the corrosive media, accelerating corrosion. Crucibles from Y-PSZ have been used as samples in experiments with various slags. We also demonstrate the use of cathodoluminescence microscopy as a powerful mapping tool for zirconia phase differentiation which was verified by Raman and XRD measurements.

Keywords: Corrosion; Spectroscopy; X-ray methods; ZrO_2; Refractories

1. Introduction

Zirconia based refractories have become more and more important to the ferrous metal industry in the last decades. Its properties - the remarkable fracture toughness, the low thermal conductivity, the excellent wear resistance and resistance to corrosive attacks of various types of slags and melts of all kinds – are in high demand. Today many components that need to tolerate strong chemical and physical attacks are made of zirconia based refractories. Sliding plates, submerged nozzles and linings of refining vessels are just a few examples for zirconia made refractories. However, Mg- and Ca-stabilized zirconia are commonly used in the metal industry,[1,2] whereas yttria stabilized zirconia is currently used as a thermal barrier coating (TBC) on turbine plates[3] to prevent physical and chemical damage caused by the bombardment and melting of inorganic, siliceous compounds like volcanic ashes, sand or dust. Today zirconia based materials are discussed as a proper substitute for carbon containing refractories particularly with regard to decrease the emission of carbon monoxide and dioxide.[4]

A well-known phenomenon in stabilized zirconia ceramics is the phase transformation from the fully stabilized cubic or the partially stabilized tetragonal phase into the monoclinic phase with an accompanied volume increase[5] of ~5% due to mechanical treatment[6] and/or the loss of the stabilizing agent.[7,8] The latter will be the phase transformation enforcing mechanism to be investigated in this study.

The corrosion mechanism of Mg- and Ca-doped zirconia refractories is well investigated.[1,2,9,10] Former studies on corrosion tests of Ca-stabilized zirconia found the infiltration of SiO_2 to be the main reason for the destabilization of zirconia.[2,11] SiO_2 and CaO form a glass of low melting point, from which pseudowollastonitic crystals precipitate (during slow cooling to room temperature) next to CaO depleted ZrO_2 grains.[9] Accordingly the Ca-stabilized cubic zirconia gets destabilized and a transformation into monoclinic zirconia occurs. The interaction of Y-stabilized zirconia with metallurgical slags is barely investigated so far. A work of Strakhov 1979[11] certifies Y_2O_3-stabilized zirconia a good corrosion resistance to siliceous melts up to 1850 °C. Other studies focused on metal melts,[12] and glasses.[13–15] Works on YSZ–TBCs in contact to calcia–magnesia–alumina–silica (CMAS) melts were done by Krämer,[3] Rai,[16] Wellman[17] and Wu[18] for instance. However, in his study Krämer has investigated the behavior of one single partially stabilized zirconia material with 7 wt.% yttria with particular attention to the interaction with fly ashes. By contrast, we will systematically investigate the corrosion behavior

* Corresponding author. Tel.: +49 7071 29 76804; fax: +49 7071 29 3060.
E-mail addresses: yannick.hemberger@uni-tuebingen.de (Y. Hemberger), christoph.berthold@uni-tuebingen.de (C. Berthold), klaus.nickel@uni-tuebingen.de (K.G. Nickel).

0955-2219/$ – see front matter © 2011 Elsevier Ltd. All rights reserved.
doi:10.1016/j.jeurceramsoc.2011.12.005

and the corrosion kinetics of yttria stabilized zirconia materials in contact to metallurgical slags, siliceous melts and liquid metals with special respect to the variance of prominent influence factors like temperature, time and chemistry of both, zirconia material and melt in further steps. One first crucible test, which is basis of the present study, has been done. Other tests with variations of zirconia crucible chemistry and slag composition will follow in the near future.

2. Experimental procedure

We have used a crucible made of 9 wt.% yttria stabilized zirconia (YSZ). The purity of this sintered material is 99.7%. 0.3% are impurities (Si, Fe, Mg) introduced by the starting powders or added as a sintering aid by the manufacturer in case of Al_2O_3. The Al_2O_3 content is supposed to be around 0.2 wt.%. The material has a density of 5.7 g/cm^3, a porosity of approximately 2.5% and small amounts of liquid phase in the triple junctions of the ZrO_2 grains. The porosity is almost completely intragranular with an average pore size of 2–3 μm. According to the manufacturer the average grain size of the YSZ-material is 50 μm. However, the photo micrographs of the YSZ-crucible after testing prove contrary. The average grain size is supposed to be only half as large (25–30 μm) as given by the manufacturer. The instant phase composition can be roughly estimated with 50–55 wt.% tetragonal and 45–50 wt.% cubic ZrO_2. A monoclinic amount can hardly be verified and is supposed to be around 1 wt.%.

The melt was a typical metallurgical slag with the main components of 60 wt.% SiO_2, 25 wt.% CaO, 7 wt.% Al_2O_3, 4 wt.% Fe_xO, 2 wt.% MgO and 2 wt.% MnO. The slag was grounded to powder and 1.5 g of the slag powder was filled in the YSZ crucible. The slag filled crucible was placed in an alumina crucible to prevent the furnace lining from damage due to a possible slag leakage. The whole assembly was fired to 1500 °C and hold for 6 h. We used a bottom loading BLF 1700 (Carbolite, Hope, UK) with a quick releasing device to be able to quench the assembly to ambient temperature in a short time to avoid crystallizations inside the slag. After cooling the assembly was cut in half and a polished cross section was prepared for further investigations.

3. Analyzing methods

We have used a conventional polarization microscope (Carl Zeiss, Oberkochen, Germany) with an attached cold cathode cathodoluminescence unit 8200 CL MK 4 (Cambridge Image technology, Cambridge, UK) and a peltier cooled CCD camera TCC-3.3ICE-N (Tucsen Imaging Technology Co., Ltd., Fujian, China). A comparable setup is described by Karakus and Moore.[19] Furthermore we have used a micro X-Ray diffractometer D8 Discover (Bruker, Karlsruhe, Germany) with focusing X-ray optics, which provide a measuring spot size down to 50 μm[20] and a 2 dimensional VÅNTEC 500 detector (Bruker, Karlsruhe, Germany, further referred to as μXRD^2). A classic X-Ray diffractometer with Bragg-Brentano geometry, a Siemens 5005 (Siemens, München, Germany) in combination with Siro-Quant 3.0 (Sietronics, Canberra, Australia) was used to estimate the instant phase composition of the YSZ material. For Raman spectroscopy we have used an InVia Reflex (Renishaw, New Mills, Gloucestershire, UK) with a green laser (532 nm) and a 1800-line grating as well as a X-Ray fluorescence spectrometer PRAXIS prototype (further referred to as μXRF). For image analyzing purpose we have used light microscopic images processed and analyzed by the computer-based LUCIA G software (Laboratory Imaging s.r.o., Prague, Czech Republic).

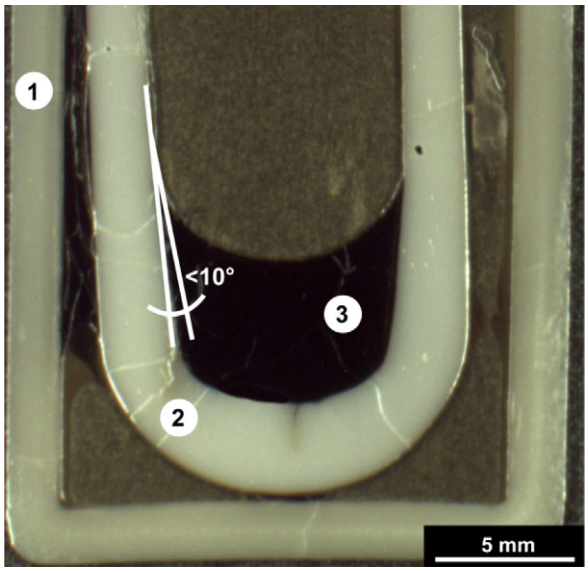

Fig. 1. Test assembly with an alumina crucible for protection purpose (1), the 8Y zirconia test crucible (2) and the slag (3) after 6 h at 1500 °C. The wetting angle is far lower than 90°. Several cracks have been formed due to the fast cooling process.

4. Results and discussion

The addition of Al_2O_3 as a sintering aid yields a reduction of the sintering temperature and an increasing densification during the sintering process.[21,22] The densification process is discussed controversially. Radford[21] wrote that the densification process is achieved by a liquid phase mechanism as seen by the grain boundary phases and rounded grain morphologies whereas Butler and Drennan[22] found most Al_2O_3-particles ending up in intragranular sites. The authors conclude that "... the Al_2O_3-particles prevent grain growth by boundary pinning for long enough that most of the porosity is eliminated before breakaway takes place."[22] Anyway there is no doubt that the main part of the Al_2O_3 additive is located in the grain boundary phases or intragranular sites rather than being integrated in the YSZ lattice because of the limited solid solubility of the Al_2O_3.[23] Therefore, the addition of a low Al_2O_3 dose has a negligible effect on the chemical stability of the actual YSZ-material but indeed does have an effect on physical properties due to the increasing density.

The wetting of the YSZ by the slag is very good. A thin film of slag even reaches the upper edge of the crucible and the wetting angle is smaller than 10° (Fig. 1). A good wetting slag is an indicator for a possible intense material–slag interaction. By analyzing the material–slag interface via light microscopy

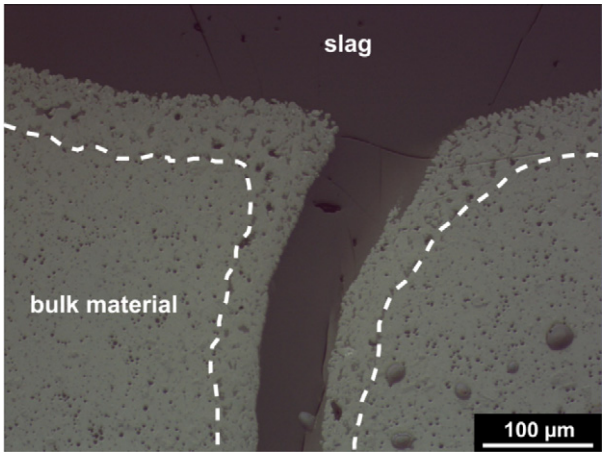

Fig. 2. Photomicrograph of the material–slag interface with an increase of porosity, a change of porosity location from intragranular (bulk material) to intergranular (affected layer) and an apparent grain coarsening in the upper layer (marked by the dashed line).

a grain coarsening and an increase in porosity became visible (Fig. 2).

The effective porosity and accordingly the porosity change in the affected material close to the slag cannot be determined by Hg-porosimetry or comparable porosimetric methods due to the completely slag infiltrated pores. In the contact area a slag filled porosity of approximately 8% was determined by image analyzing techniques emphasizing the first visual impression via light microscopy. The used image analyzing techniques are described elsewhere.[24] The porosity changes from intragranular (starting material) into intergranular (affected contact layer).

Due to the sensitivity to very small variations in chemistry and structural changes cathodoluminescence microscopy (further referred to as CLM) can provide further information about structural and/or chemical changes.[19,24–28] The blue luminescent contact area (Fig. 3) can be distinguished very easily from the red luminescent unaffected bulk material.

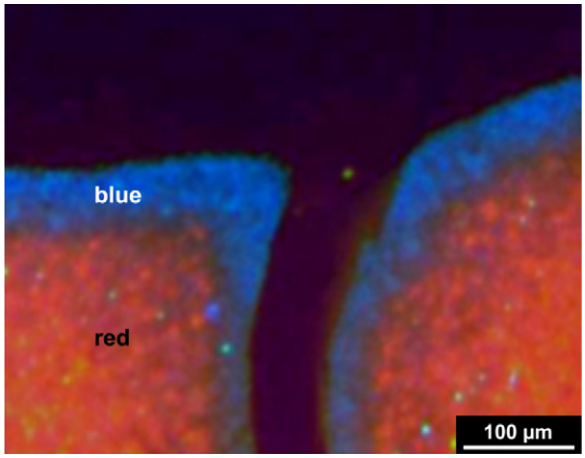

Fig. 3. CLM image of the same area as shown in Fig. 2. The unaffected bulk material shows a red luminescence color from which the blue luminescent contact area can be distinguished very easily. The slag shows no luminescence effect.

Baddeleyite, the only natural and monoclinic ZrO_2 modification, and artificial monoclinic zirconia are both well known for their blue cathodoluminescence,[19,29] eventhough the cause for this blue color is discussed controversially. Several authors[30] designate intrinsic (lattice) defects like O^{2-} vacancies, which are proposed to accommodate stabilizing cations, or the stabilizing cations themselves to be the reason for the blue luminescence color. In contrast, Sarver[31] promoted small TiO_2 impurities to cause a blue luminescence color in monoclinic zirconia. However, Karakus[32] mentioned O^{2-} vacancies to be responsible for brilliant whitish cathodoluminescence colors whereas TiO_6-defects are supposed to be responsible for greenish colors in baddeleyite.

In contrast to monoclinic zirconia, tetragonal and cubic zirconia hardly show any luminescence.[30,33] The red luminescence color of the bulk material in this study can be attributed to small amounts of alumina[19] situated at grain boundary[21] or intragranular sites[22] as a result of the limited solid solubility of Al_2O_3 in YSZ.[23]

Nonetheless the obvious differences in luminescent colors suggest that an interaction between the YSZ and the slag has occurred which lead to chemical and/or structural changes inside the YSZ and accordingly to a change in slag chemistry.

To analyze the structural changes we have conducted μXRD^2 measurements. The measuring spot is elliptical with a diameter of $\sim 200\,\mu m \times 50\,\mu m$ (depending on the incidence angle). A comparable μXRD^2 setup with slight hardware configurations is described by Berthold et al.[20] A first measurement in the bulk material shows only tetragonal zirconia in the diffraction pattern (Fig. 4a), as was expected because of the chemical composition of the starting YSZ material.[34,35] The diffraction pattern of monoclinic zirconia becomes visible (Fig. 4c) inside the zone with blue luminescence. From detailed line scans we know that the amount of monoclinic zirconia is increasing and the amount of tetragonal zirconia is decreasing toward the material–slag interface.

Due to the 2D-detector we are also able to make reliable statements about the crystal size of the material. The phase transformation from t-ZrO_2 to m-ZrO_2 has been reported to be accompanied by an increase in grain size.[36] However, a decrease in crystal size is indicated by our diffraction patterns (Fig. 4b and d). The spotty t-ZrO_2 diffraction rings identify a coarse crystallite size in contrast to the more finely dispersed spots in diffraction rings of the monoclinic zirconia. We attribute this to the formation of monoclinic twins and an accompanied crystallite size refinement during the t-ZrO_2 to m-ZrO_2 phase transformation (Fig. 5).

We were not able to resolve the total depth of phase transformation by using μXRD^2 because the measuring spot was still too big to resolve the transformation zone. To do more precise measurements with a better spatial resolution we conducted Raman spectroscopy. By using a mapping tool we were able to analyze the total depth of penetration and the phase distribution of the contact area. The penetration depth was found to be 50–80 µm (Fig. 6).

This is in agreement with the CLM results. Obviously the monoclinic ZrO_2 is homogeneously distributed all over the

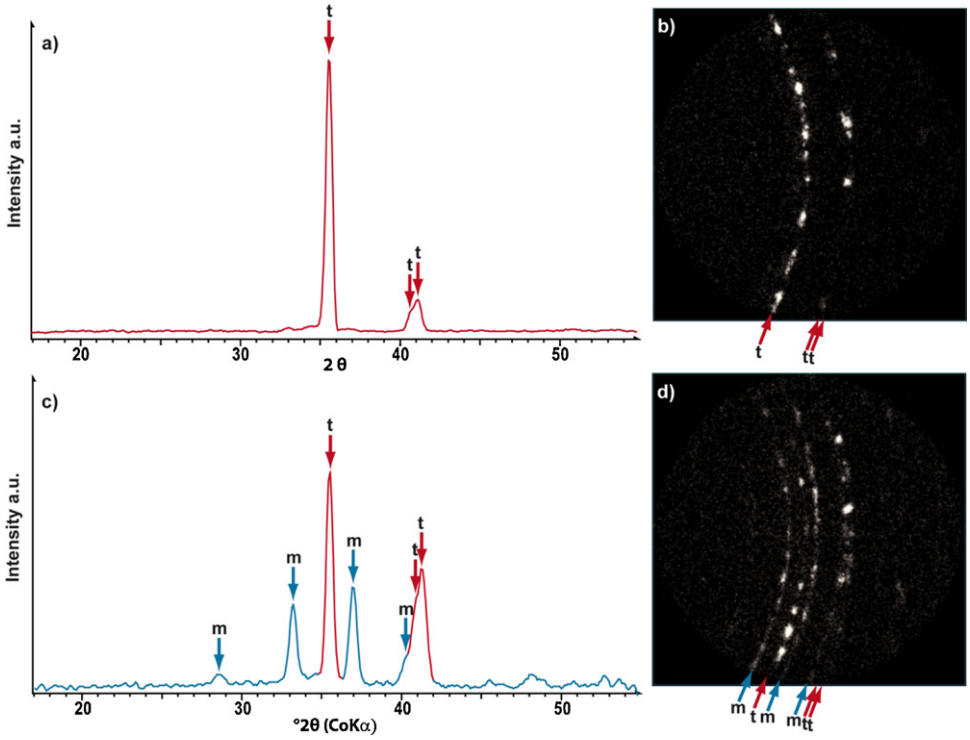

Fig. 4. The figure shows two μXRD[2] pattern with associated diffraction rings of the red luminescent (a + b) and the blue luminescent area (c + d). Pattern (a) is totally tetragonal with a large crystal size that can be seen by the coarse, unevenly distributed diffraction rings in (b). By contrast, the diffraction pattern (c), which was taken in the blue luminescent area in addition, shows large amounts of monoclinic zirconia. The monoclinic diffraction rings are much finer and distributed more evenly what is an indication for smaller crystal sizes.

contact area but there is a transition zone between the bulk material and the transformed area, in which the amount of m-ZrO_2 decreases toward the inner material. In contrast to the assumption, that the tetragonal phase will entirely transform into the monoclinic modification the phase transformation from t-ZrO_2 to m-ZrO_2 was incomplete. A small amount of t-ZrO_2 is still detectable even next to the material–slag interface (Fig. 7).

To investigate the reason for the phase transformation we have analyzed the chemistry along the profile AB (Fig. 8) inside the bulk material, across the interface and in the slag by μXRF. The first element that can be detected and quantified by μXRF is Ca. Elements lighter than Si cannot be detected and elements lighter than Ca cannot be quantified accurately without a vacuum chamber. Hence, electron microprobe measurements will be done as a next step to analyze the distribution and the quantity of SiO_2, CaO and Al_2O_3 inside the YSZ. All of these components are main parts of the slag and especially SiO_2 is well known as a destabilization agent for stabilized zirconia.[1,2,11,37]

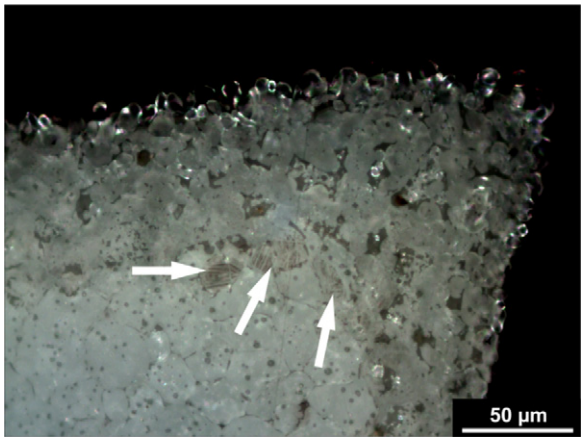

Fig. 5. RLM photomicrograph taken with crossed polarizers. One possible explanation for the decrease in crystal size during the transformation process from tetragonal to monoclinic zirconia is the formation of monoclinic twins (marked by white arrows).

In Kato's[15] opinion the presence of CaO in corroding melts has a strong impact on the corrosion, especially on the ZrO_2-dissolution into the melt. He supposed that the CaO makes the structure of the glass/melt desirable for the transport of Zirconium in the glass/melt.

Fe_2O_3 and MnO are supposed to be zirconia corrosion catalyzers. An increasing Fe_2O_3 content will rise the mobility of the slag, which increases the contact surface between melt and refractory (improves the wetting) which in turn intensifies the interaction of silica and stabilized zirconia.[11] Strakhov and Zhukovskaya have also shown that an increase in MnO content in the melt intensifies the corrosion of stabilized zirconia.

We found Fe, Mn and Ca infiltrating into the YSZ and Y, the stabilizing agent, leaching into the slag in a significantly greater amount than Zr dissolved in the slag. The increasing intergranular porosity inside the transformed area (Fig. 2) is supposed to be related to the dissolution of the destabilized, more soluble monoclinic zirconia[38] into the slag while the disappearance of intragranular porosity could be due to the phase transformation

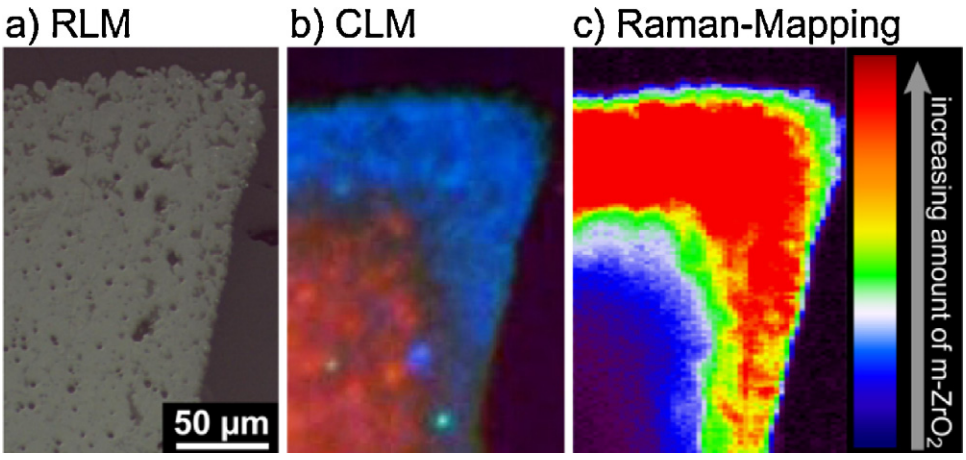

Fig. 6. The same sample area analyzed by RLM (a), CLM (b) and Raman-mapping (c). There are no differences between contact area and bulk material in the RLM image but obvious differences in the CLM image. The contact area is supposed to be transformed into m-ZrO_2 because m-ZrO_2 is well known for its bluish luminescence color. The Raman analysis confirmed this assumption.

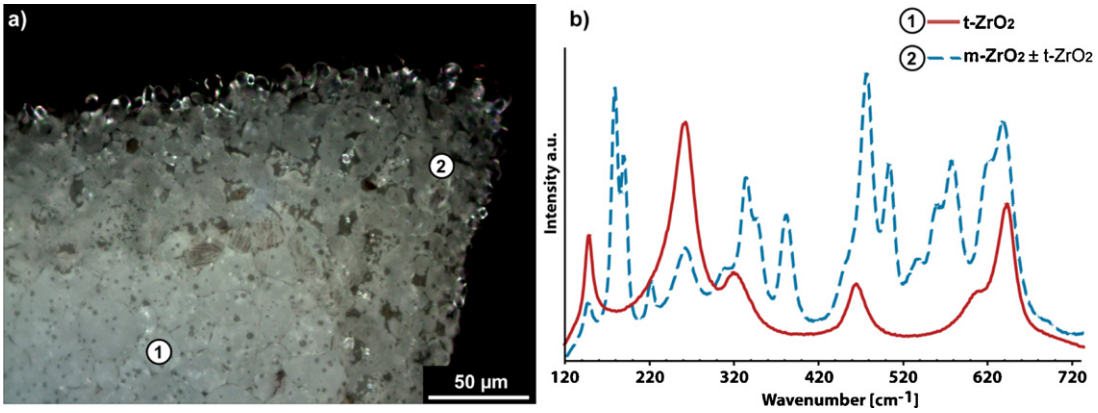

Fig. 7. Photomicrograph of the contact area (see Fig. 5) with marked Raman measuring points (a) and the corresponding Raman spectra (b) of pure t-ZrO_2 (1) and m-ZrO_2 with small amount of t-ZrO_2 (2).

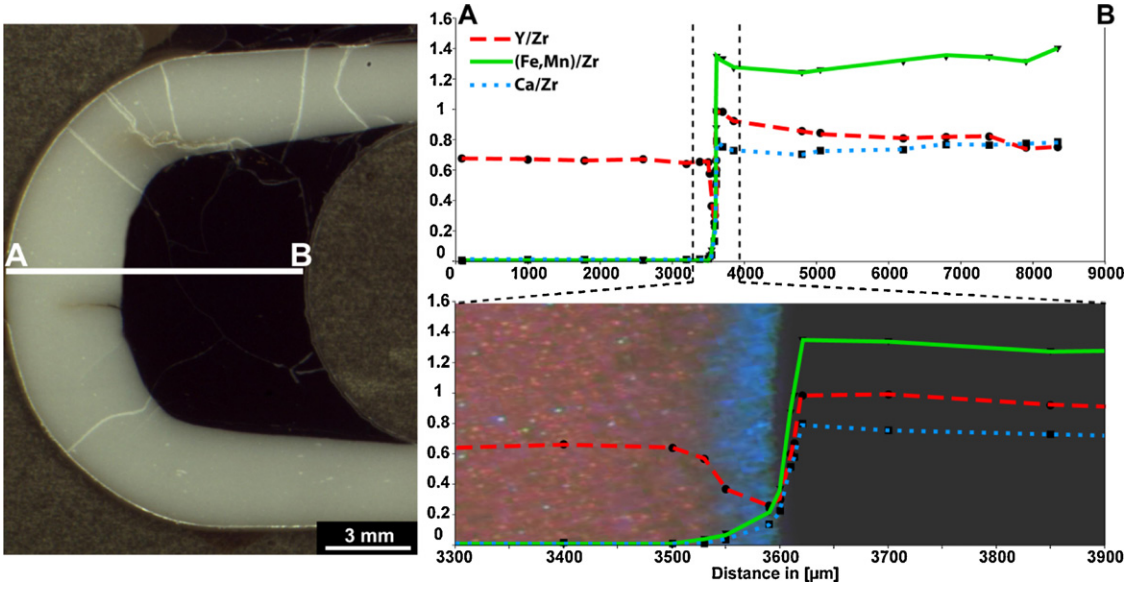

Fig. 8. Photomicrograph of the slag-filled crucible with marked A–B profile line (left side), the chemical profile from A to B with the corresponding Y/Zr, (Fe, Mn)/Zr and Ca/Zr ratios (upper right side) and a magnification of the profile around the material–slag contact area (lower right side).

of t-ZrO_2 into m-ZrO_2 and its inherited volume expansion of almost 5%.[5]

The infiltration and leaching/dissolution process were found to be restricted to the upper 50–80 μm. This is in agreement with the discovered transformation depth. Obviously the loss of the stabilizing agent yttria below a certain extent causes the transformation into monoclinic Zirconia. After Scott (1975) the critical Yttria-content below which only the monoclinic phase is stable is around 3mol% of $YO_{1.5}$ (∼3 wt.% Y_2O_3). Next to the material–slag interface we have measured a Y_2O_3 content of ∼2 wt.% and in the transition zone to the unaffected bulk material a content of approximately 3 wt.% Y_2O_3. These measurements are in agreement with Scott.[34] From to the Raman results shown in Fig. 7 we suppose that there are some grains inside the contact area, which are still tetragonal and accordingly with Y_2O_3 contents higher than 3 wt.%. Consequently there need to be lots of monoclinic grains with a Y_2O_3 content far lower than 2 wt.% because the μXRF measurements, with a measuring spot size of several μm^2, represent an average of the Y_2O_3 content of the contact area.

We fully agree with Strakhov,[11,37] Oki[9] and other workers[1,39,40] that the SiO_2 is probably the most corrosive ingredient in siliceous melts because of its affinity to form silicate melts and phases with the stabilizing agent. Some workers[41,42] found that SiO_2, from impurities in the starting zirconia material, and Y_2O_3 form Y_2SiO_4 and, in presence of Na_2O, sodium–yttria–silicates in temperature fields around 1300–1500 °C. But we still need to proof the exact corrosion mechanism of Y_2O_3-stabilized ZrO_2 in contact to siliceous melts.

Another very likely phase formation, that is described many times in case of zirconia refractories in contact to calcareous siliceous melts,[11,13,15] is the formation of calcium zirconate ($CaZrO_3$).

No recrystallizations or formations of other phases, which have been reported as decomposition products of YSZ and slag components,[9,11,13,15,41,42] were found. Considering the given CaO/ZrO_2 ratio (0.42) of the juvenile slag and the dissolved ZrO_2 amount of the slag after testing there have to be phase formations of zircon ($ZrSiO_4$) and a calcium–zirconium–silicate ($Ca_2ZrSi_4O_{12}$).[43] None of those phases were observed in our test specimen. This might be due to the relative short dwell time and/or the fast quenching process from 1500 °C to ambient temperature in just a few minutes. As shown by Barbieri et al.[44] due to kinetics no crystalline phases were formed after sintering a comparable melt/glass with subsequent air and water cooling down to room temperature. We plan to elucidate this effect in further tests by varying temperature, dwell time and quenching process.

The corrosiveness of the slag is increased by viscosity-reducing components like Fe_2O_3 and MnO. The low-viscosity melt is entering the material via pores, micro cracks or even along grain boundaries and leaches the stabilizing Y_2O_3 out of the material.The infiltration depth, which is in our case synonymous with the transformation zone (Fig. 8), depends on several variables. Slag and materials chemistry and the temperature influence the wettability and the viscosity, and the yttria- and zirconia-saturation values of the slag. If the slag gets saturated in yttria and zirconia, the leaching or dissolution of these components will stop[15] and the transformation of the t-ZrO_2 into m-ZrO_2 will not proceed further. The peak in the chemical profile of the Y/Zr ratio in Fig. 8 (upper right) at the material–slag interface and the slight decrease of the Y/Zr ratio toward the slag surface are probably the result of an incomplete intermixing of the slag, which might be attributed to the short dwell time. The Y/Zr peak probably represents a yttrium and zirconium saturated layer, which is, in combination to the badly intermixing conditions, a barrier for further corrosion, as described by Kato.[15] To verify these assumptions saturation experiments need to be done. The saturation experiments are also indispensable for making reliable statements about the leaching/dissolution potential of the slags and possibly corresponding changes in their wetting behavior.

5. Conclusion and outlook

The interaction of the zirconia material and the metallurgical slag causes a phase transformation from tetragonal into monoclinic zirconia. When the decrease of the Yttria content of the PSZ material due to the leaching of the stabilizing agent into the slag reaches a critical value of <3 wt.% the partially stabilized tetragonal zirconia transforms into monoclinic zirconia. We were able to analyze the transformation zone and determine the penetration depth of the slag into the material by using μXRD^2, Raman, μXRF and CLM.

CLM is a fast and powerful method when it comes to the analysis of zirconia refractory corrosion mechanism and high-temperature material–slag interactions in general. Due to its sensitivity to small chemical and structural variations CLM can give an overview over the phase distribution in a very short time without special requirements for sample preparations.

In the analysis of refractory-melt interactions it can be used as a pathfinder for subsequent analyzing methods as shown in this study. The bluish luminescent monoclinic zirconia can be separated very easily from the tetragonal bulk material. By using Raman and μXRD^2 we were able to confirm the adjudgements from the CLM image that the contact area transformed into monoclinic zirconia.

The results of the μXRD^2 measurements indicate a grain refinement when t-ZrO_2 transforms into m-ZrO_2. This effect can be attributed to the formation of monoclinic twins and an according decrease in crystallite size during the transformation.

The change in chemistry is restricted to the transformation zone and the slag as shown by μXRF measurements. Fe, Mn and Ca infiltrate the material and Y and Zr were leached into the slag. Si, Al and Mg cannot be detected by our μXRF due to a measurement under ambient conditions without using a vacuum chamber. From these elements especially Si is supposed to play an important role in the destabilization process. Therefore electron microprobe measurements are required to analyze the distribution of these elements and to discover their role in the destabilization and transformation process.

An important factor that will affect the material–slag interaction is the wetting behavior of the slag or the liquid phase in

general. This behavior strongly depends on the chemical composition of the liquid phase and the refractory material respectively. Therefore crucible tests with varying slag compositions will be done in a further step as well as crucible tests made of zirconia materials with different dopant contents. It is also expected that the dissolution of the bulk material and the infiltration of the liquid phase will have an impact on the wetting behavior. This dependency will be investigated by performing separate wetting tests in a hot stage microscope.

Acknowledgements

The authors would like to thank Indra Gill-Kopp for an excellent sample preparation, Barbara Meier and Norbert Walker for providing excellent technical support, Melanie Keuper for her assistance in performing Raman- and μXRF measurements, Nadja Huber for performing the μXRD^2 analysis and Verena Krasz for proof reading. Funding by DFG under Ni-299/21-1 is greatly acknowledged.

References

1. Aiba Y, Oki K, Sugie M, Kurihara K, Oya S. Study of corrosion and penetration of zirconia refractories by molten steel and slag III. *Taikabutsu Overseas* 1985;**5**:3–11.
2. Oki K, Sugie M, Kurihara K, Aiba Y, Maeda T. Study of corrosion and penetration of zirconia refractories by molten steel and slag I. *Taikabutsu Overseas* 1983;**3**:3–11.
3. Krämer S, Yang J, Levi CG, Johnson CA. Thermochemical interaction of thermal barrier coatings with molten CaO–MgO–Al_2O_3–SiO_2 (CMAS) deposits. *Journal of the American Ceramic Society* 2006;**89**: 3167–75.
4. Aneziris CG, Klippel U, Schärfl W, Stein V, Li Y. Functional refractory material design for advanced thermal shock performance due to titania additions. *International Journal of Applied Ceramic Technology* 2007;**4**:481–9.
5. Ruff O, Ebert F. Beiträge zur keramik hochfeuerfester stoffe. I. Die formen des zirkondioxyds. *Zeitschrift für anorganische und allgemeine Chemie* 1929;**180**:19–41.
6. Murase Y, Kato E. Phase transformation of zirconia by ball-milling. *Journal of the American Ceramic Society – Discussions and Notes* 1979:527.
7. Berezhnoy AS, Karyakin LI. Structure and properities of MgO–ZrO_2–SiO_2 system. *Ogneupory* 1952:211–21.
8. Berezhnoy AS, Kordyuk RA. The CaO–MgO–ZrO_2–SiO_2 system and its significance in the production of refractories. *Refractories and Industrial Ceramics* 1962;**3**:69–73.
9. Oki K, Sugie M, Kurihara K, Aiba Y, Maeda T. Study on corrosion and penetration of zirconia refractories by molten steel and slag II. *Taikabutsu Overseas* 1984;**4**:42–8.
10. Aneziris CG, Pfaff EM, Maier HR. Corrosion mechanisms of low porosity ZrO_2 based materials during near net shape steel casting. *Journal of the European Ceramic Society* 2000;**20**:159–68.
11. Strakhov VI, Zhukovskaya AE. Slag-resistant products made from stabilized ZrO_2. *Refractories and Industrial Ceramics* 1979;**20**:184–8.
12. Durov A, Naidich Y, Kostyuk B. Investigation of interaction of metal melts and zirconia. *Journal of Materials Science* 2005;**40**:2173–8.
13. Suk MO, Park JH. Corrosion behaviors of zirconia refractory by CaO–SiO_2–MgO–CaF_2 slag. *Journal of the American Ceramic Society* 2009;**92**:717–23.
14. Rahimi RA, Ahmadi A, Kakooei S, Sadrnezhaad SK. Corrosion behavior of ZrO_2–SiO_2–Al_2O_3 refractories in lead silicate glass melts. *Journal of the European Ceramic Society* 2011;**31**:715–21.
15. Kato K, Araki N. The corrosion of zircon and zirconia refractories by molten glasses. *Journal of Non-Crystalline Solids* 1986;**80**:681–7.
16. Rai AK, Bhattacharya RS, Wolfe DE, Eden TJ. CMAS-resistant thermal barrier coatings (TBC). *International Journal of Applied Ceramic Technology* 2010;**7**:662–74.
17. Wellman R, Whitman G, Nicholls JR. CMAS corrosion of EB PVD TBCs: identifying the minimum level to initiate damage. *International Journal of Refractory Metals and Hard Materials* 2010;**28**: 124–32.
18. Wu J, Guo H-B, Gao Y-Z, Gong S-K. Microstructure and thermo-physical properties of yttria stabilized zirconia coatings with CMAS deposits. *Journal of the European Ceramic Society* 2011;**31**:1881–8.
19. Karakus M, Moore RE. CLM – a new technique for refractories. *American Ceramic Society Bulletin* 1998;**77**:55–61.
20. Berthold C, Bjeoumikhov A, Brügemann L. Fast XRD^2 microdiffraction with focusing X-ray microlenses. *Particle & Particle Systems Characterization* 2009;**26**:107–11.
21. Radford KC, Bratton RJ. Zirconia electrolyte cells. *Journal of Materials Science* 1979;**14**:59–65.
22. Butler EP, Drennan J. Microstructural analysis of sintered high-conductivity zirconia with Al_2O_3 additions. *Journal of the American Ceramic Society* 1982;**65**:474–8.
23. Lakiza SM, Lopato LM. Stable and metastable phase relations in the system alumina–zirconia–yttria. *Journal of the American Ceramic Society* 1997;**80**:893–902.
24. Hemberger Y, Presser V, Berthold C, Nickel KG. Kathodolumineszenzmikroskopie: Eine schnelle, leistungsstarke methode zur analyse von feuerfestmaterialien. In: Kriegesmann J, editor. *Technische keramische werkstoffe*. Köln: Deutscher Wirtschaftsdienst; 2011. p. 1–60 [Kap. 6.1.2.1].
25. Marfunin AS. *Spectroscopy, luminescence and radiation centers in minerals*. Heidelberg: Springer Verlag; 1979.
26. Smith JV, Stenstrom RC. Electron-excited luminescence as a petrologic tool. *Journal of Geology* 1965;**73**:627–35.
27. Götze JU. *Cathodoluminescence microscopy and spectroscopy in applied mineralogy*. Freiberg: Technische Universität Bergakademie Freiberg; 2000.
28. Marshall DJ. *Cathodoluminescence of geological materials*. London: Unwin Hyman Ltd.; 1988.
29. Keil K, Fricker PE. Baddeleyite (ZrO_2) in gabbroic rocks from axel Heiberg island, Canadian arctic archipelago. *American Mineralogist* 1974;**59**:249–53.
30. Czeknuszka JT, Page TF. Cathodoluminescence: a microstructural technique for exploring phase distributions and deformation structures in zirconia ceramics. *Journal of the American Ceramic Society* 1985;**68**. C-196–9.
31. Sarver JF. Preparation and luminescent properties of Ti-activated zirconia. *Journal of The Electrochemical Society* 1966;**113**: 124–8.
32. Karakus M. Cathodoluminescence properties of raw minerals used in refractory ceramics. *Refractories Applications and News* 2005;**10**:16–9.
33. Leach C, Norman CE. Spectroscopic cathodoluminescence studies of Mg-PSZ. *Journal of Materials Science* 1992;**27**:4219–22.
34. Scott HG. Phase relationships in the zirconia–yttria system. *Journal of Materials Science* 1975;**10**:1527–35.
35. Ingel RP, Lewis DI. Lattice parameters and density for Y_2O_3-stabilized ZrO_2. *Journal of the American Ceramic Society* 1986;**69**: 325–32.
36. Chevalier J, Gremillard L, Deville S. Low-temperature degradation of zirconia and implications for biomedical implants. *Annual Review of Materials Research* 2007;**37**:1–32.
37. Strakhov VI, Zhukovskaya AE, Sergeev GG, Shmitt-Fogelevich SP. Interaction of stabilized ZrO_2 with silica. *Refractories and Industrial Ceramics* 1974;**15**:701–4.
38. Chung YD, Schlesinger ME. Interaction of CaO–FeO–SiO_2 slags with partially stabilized zirconia. *Journal of the American Ceramic Society* 1994;**77**:611–6.
39. Mallinckrodt DV, Reynen P, Zografou C. The effect of impurities on sintering and stabilization of ZrO_2 (CaO). *Interceram* 1982;**31**:126.
40. Dupre B, Gleitzer C, Le Coq X, Kaerle MC, Guenard C. Decalcification of stabilized zirconia by silica and some other

oxides. *Journal of the European Ceramic Society* 1992;**9**: 389–95.

41. Badwal SPS, Hughes AE. The effects of sintering atmosphere on impurity phase formation and grain boundary resistivity in Y_2O_3-fully stabilized ZrO_2. *Journal of the European Ceramic Society* 1992;**10**:115–22.
42. Hughes AE, Sexton BA. XPS study of an intergranular phase in yttria–zirconia. *Journal of Materials Science* 1989;**24**:1057–61.
43. Tanaka K, Maekawa M, Obata T, Tamaki N, Nakazawa Y. The compatibility relationships in the system ZrO_2–CaO–SiO_2 at 1400–1500 °C. *Journal of the Ceramic Society of Japan (Yogy o-ky okai-shi)* 1985;**93**: 418–25.
44. Cannillo V, Leonelli C, Montorsi M, Mustarelli P, Siligardi C. Experimental and MD simulations study of CaO–ZrO_2–SiO_2 glasses. *The Journal of Physical Chemistry B* 2003;**107**:6519–25.